Icarus 287 (2017) 37–46

Contents lists available at ScienceDirect

Icarus

journal homepage: www.elsevier.com/locate/icarus

Long-term surface temperature modeling of Pluto

Alissa M. Earle[a,*], Richard P. Binzel[a], Leslie A. Young[b], S.A. Stern[b], K. Ennico[c], W. Grundy[d], C.B. Olkin[b], H.A. Weaver[e], the New Horizons Geology and Geophysics Imaging Team

[a] Department of Earth, Atmospheric, and Planetary Sciences, Massachusetts Institute of Technology, Cambridge, Massachusetts 02139, US
[b] Southwest Research Institute, Boulder, CO 80302, USA
[c] National Aeronautics and Space Administration (NASA) Ames Research Center, Space Science Division, Moffett Field, CA 94035, USA
[d] Lowell Observatory, Flagstaff, AZ 86001, USA
[e] Johns Hopkins University Applied Physics Laboratory, Laurel, MD 20723, USA

ARTICLE INFO

Article history:
Received 6 February 2016
Revised 15 September 2016
Accepted 21 September 2016
Available online 29 September 2016

Keywords:
Pluto
Pluto
atmosphere
Pluto
surface

ABSTRACT

NASA's New Horizons' reconnaissance of the Pluto system has revealed at high resolution the striking albedo contrasts from polar to equatorial latitudes on Pluto, as well as the sharpness of boundaries for longitudinal variations. These contrasts suggest that Pluto must undergo dynamic evolution that drives the redistribution of volatiles. Using the New Horizons results as a template, we explore the surface temperature variations driven seasonally on Pluto considering multiple timescales. These timescales include the current orbit (248 years) as well as the timescales for obliquity precession (peak-to-peak amplitude of 23° over 3 million years) and regression of the orbital longitude of perihelion (3.7 million years). These orbital variations create epochs of "Extreme Seasons" where one pole receives a short, relatively warm summer and long winter, while the other receives a much longer, but less intense summer and short winter. We use thermal modeling to build upon the long-term insolation history model described by Earle and Binzel (2015) and investigate how these seasons couple with Pluto's albedo contrasts to create temperature effects. From this study we find that a bright region at the equator, once established, can become a site for net deposition. We see the region informally known as Sputnik Planitia as an example of this, and find it will be able to perpetuate itself as an "always available" cold trap, thus having the potential to survive on million year or substantially longer timescales. Meanwhile darker, low-albedo, regions near the equator will remain relative warm and generally not attract volatile deposition. We argue that the equatorial region is a "preservation zone" for whatever albedo is seeded there. This offers insight as to why the equatorial band of Pluto displays the planet's greatest albedo contrasts.

1. Introduction

NASA's New Horizons mission has provided a wealth of new data about the Pluto system, including detailed surface geology and volatile distribution maps (Grundy et al., 2016; Stern et al., 2015). The images of Pluto sent back by New Horizons also reveal striking latitudinal and longitudinal albedo variations on Pluto's surface (Grundy et al., 2016; Stern et al., 2015) bringing to high resolution the intriguing variegation originally revealed from Earth through decades of mapping efforts (e.g. Buie and Tholen, 1989; Buie et al., 2010; Young and Binzel, 1993; Grundy et al., 2013). These features provide new motivation for studying surface temperature variations on Pluto both in the current epoch as well as over the past few million years as Pluto's orbit has undergone variations creating dramatic differences in Pluto's seasons over million year timescales.

Pluto's long-term seasonal variations are driven by two factors: Pluto's longitude of perihelion regresses through 360° over 3.7 million years while its obliquity varies over a total range of ~23° over a period of 3 million years (Dobrovolskis and Harris, 1983). Pluto's changing obliquity and regression of perihelion create variations in its sub-solar latitude at perihelion spanning from +77° to −53° over the past 3 million years (Fig. 1).[1] Since Pluto has a high orbital eccentricity ($e \approx 0.25$) its heliocentric distance ranges between roughly 30 AU and 50 AU, which leads to the solar

* Corresponding author.
E-mail addresses: aearle@mit.edu, alissaearle@gmail.com (A.M. Earle).

http://dx.doi.org/10.1016/j.icarus.2016.09.036
0019-1035/

[1] We use the current IAU convention of defining "north" according to the direction of Pluto's angular momentum vector.

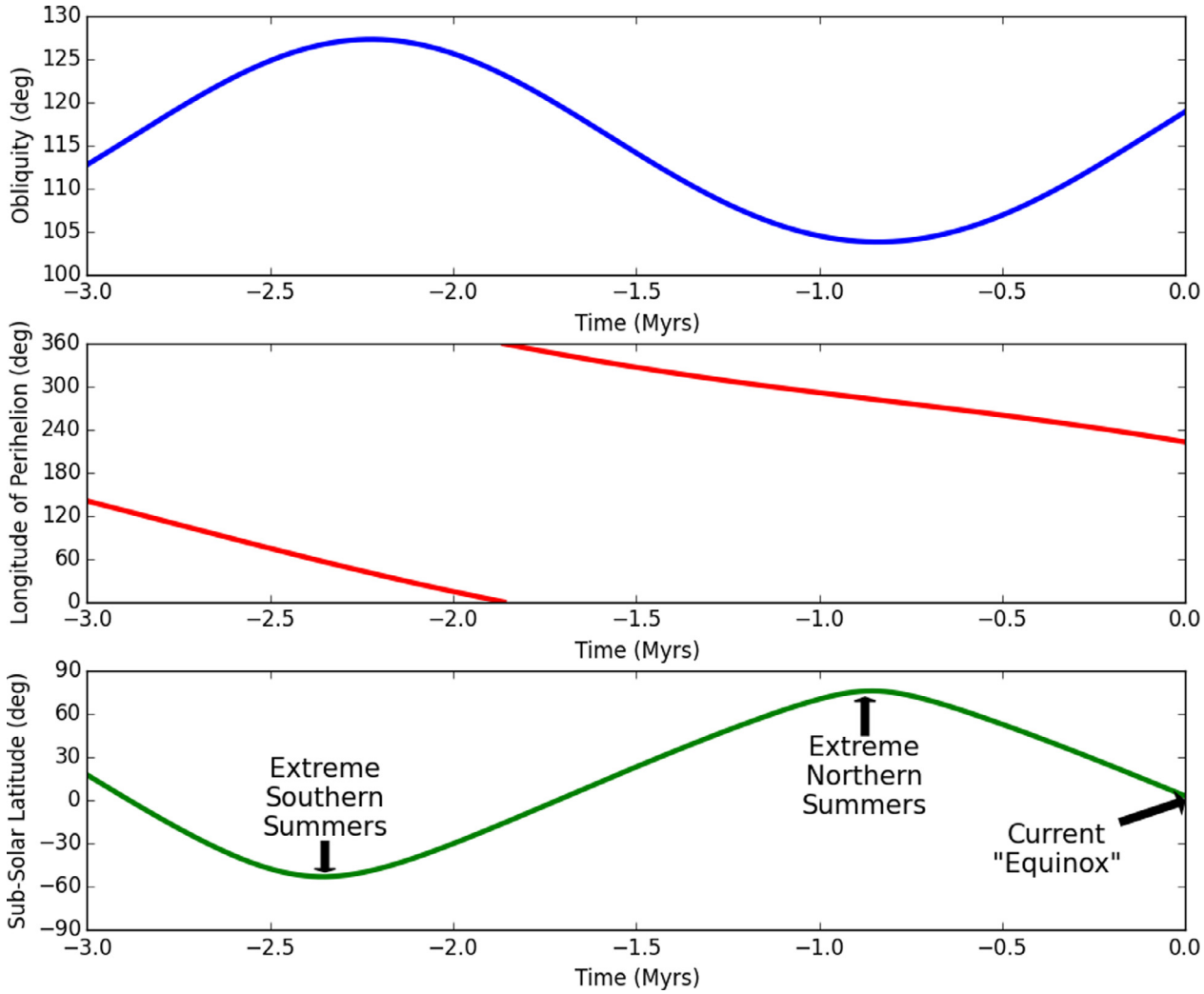

Fig. 1. This figure is adapted from Earle and Binzel (2015). **Top:** Pluto's obliquity variations as a function of time over the last 3 million years. The period of obliquity oscillations is 2.8 million years. **Middle:** Pluto's regressing longitude of perihelion as a function of time. It takes 3.7 million years for Pluto's longitude of perihelion to regress a full 360° **Bottom:** Sub-solar latitude at perihelion as a function of time. Based on Dobrovolskis et al. (1997) and Dobrovolskis and Harris (1983). This figure originally appeared in Earle and Binzel (2015).

constant varying by a factor of ~3 between perihelion and aphelion (van Hemelrijck, 1982; Spencer et al., 1997). This dramatic difference between perihelion and aphelion when combined with periods of Pluto having a high sub-solar latitude at perihelion (for example, during the two time periods labeled in Fig. 1) creates epochs of "Extreme Seasons" where one pole experiences a very short, intense summer and long winter, while the other has a short winter, and longer, but less intense summer season. Here we set out to determine what effect these "Extreme Seasons" as well as Pluto's albedo variations have on Pluto's surface temperatures. The impact on atmospheric pressure and possible implications for surface morphology are addressed by Stern et al. (2015). In this work we focus on the asymmetric surface temperature effects of these changing geometries as opposed to the effects of total accumulated insolation. Previous work (e.g. Earle and Binzel, 2015) focused on pole-to-pole insolation asymmetries, but those asymmetries are now shown not to be correct. Full accounting for the Keplerian slowing of the orbital velocity near aphelion was not adequately modeled by Earle and Binzel (2015). Nadeau and McGehee (2015) and Hamilton (2016, submitted) show that the slowly changing aspect angle at aphelion compensates for the greater heliocentric distance and balances out the pole-to-pole accumulated insolation over a single orbit. While insolation is symmetric, here we find that maximum surface temperature, being a much more instantaneous effect, proves to be both asymmetric and a greater driver of volatile transport activity. Thus our focus on temperature modeling in the present work.

Previous work has already been done to model volatile transport on Pluto (and inherently surface temperature). With the exception of Young et al. (2015), most of this work predates the New Horizons' flyby of the Pluto system so their only observational constraints are atmospheric measurements from occultation observations and lower resolution ground-based albedo maps (Hansen et al., 2015; Olkin et al., 2015; Young, 2013). These works also all focus on the current epoch. We try to build upon the previous work by making use of the results from NASA's New Horizons mission as well as considering the long term variations in Pluto's orbit and resultant "Extreme Seasons". Pluto's orbit is believed to be chaotic on timescales of 10–20 million years (Sussman and Wisdom, 1988; 1992). Here we focus on timescales of 3 million years or less in order to stay well below the limit of Pluto's orbit becoming chaotic. Further discussion of Pluto's orbital chaos, and its possible impact on our results can be found in the introduction of Earle and Binzel (2015).

2. Methods

2.1. Local temperature model

A first step towards understanding seasonal surface temperatures is looking at the annual insolation averages and how they vary over million year timescales. To do this we start by calculating Pluto's orbit over the timescales of interest using the orbital model of Pluto initially presented in Dobrovolskis and Harris (1983) and refined in Dobrovolskis et al. (1997). This model well represents Pluto's orbit for time scales of 10 million years, which is several times the length of our longest trial making this model sufficiently accurate for our purposes (Dobrovolskis et al., 1997). This provides us with the inputs necessary to calculate Pluto insolation as a function of latitude using the equations found in Levine et al. (1977) and an updated orbitally symmetric model from Earle and Binzel (2015) as guided by the analytic solution by Nadeau and McGehee (2015) and discussed by Hamilton (2016, submitted).

We choose to focus on three significant epochs in Pluto's orbital history. The first is Pluto's current orbit, characterized by equinox and perihelion occurring close together. Second is Pluto's orbital geometry 0.9 million years ago, characterized by Pluto's sub-solar point at perihelion being high in the northern hemisphere; we call this "extreme northern summer". The third epoch of interest is Pluto's orbital geometry 2.35 million years ago, characterized by Pluto's sub-solar latitude at perihelion being low in the southern hemisphere; we call this "extreme southern summer".

We begin comparing these epochs by examining the insolation averaged over one Pluto orbit (Fig. 2, top left panel). At the current epoch (blue, solid line) one Pluto orbit yields insolation maxima at the poles and minima around ±30° (Earle and Binzel, 2015). During the epoch 0.9 million years ago (green, dashed line), the equator received a substantially lower minimum value for its insolation while the poles received almost 1.5 times as much insolation on average. For the epoch 2.35 million years ago, (purple, dotted line), a relatively flat latitudinal insolation pattern emerges with the maximum occurring at the equator, with additional local maxima at each pole, and minima just beyond ±30°. During the current epoch, characterized by equinox occurring near perihelion and aphelion, both poles receive relatively similar insolation patterns. However during past epochs when Pluto underwent what we call "extreme seasons" one pole received more insolation over a shorter period of time while the other received less insolation but for a longer stretch of time, creating asymmetries in the maximum insolation as a function of latitude (Fig. 2). These differences between maximum insolation and duration of time over which it is received become relevant when trying to model surface temperatures during different epochs.

While the average annual insolation and average surface temperature (Fig. 2 top left and bottom left, respectively) show pole-to-pole symmetry, the maximum local insolation and surface temperatures reached show the asymmetries that we call "extreme seasons". In order to calculate surface temperatures as a function of latitude and albedo we use the 1-dimensional thermophysical model presented in Spencer et al. (1989) (all temperatures calculated and presented herein are surface temperatures, unless otherwise indicated). The Spencer model was designed to calculate surface and subsurface temperatures on a rotating body as a function of local time and was originally written in IDL, but here has been rewritten in Python and adapted for seasonal changes corresponding to the varying sub-solar latitude and heliocentric distance. The model determines heating in the surface layer by balancing thermal emission, insolation, and conduction with the layer below. The middle layers are balanced by conduction only from the layer above and below. The bottom layer is balanced by conduction with the layer above and the lower boundary heat flux (Spencer et al., 1989). For the lower boundary heat flux we use 2.5 ergs/cm^{2}s. We assume an emissivity of 0.9 based on Spencer et al. (1989). For the other thermal parameters we used values for methane at 40 K given in Spencer and Moore (1992); a heat capacity of 1.8×10^7 ergs/gK, density 0.52 g/cm^3, thermal inertia 6.3×10^5 ergs/cm$^2\sqrt{s}$K.

The original version of the model is designed to calculate local temperatures over timespans of a few rotations with a constant sub-solar latitude and heliocentric distance. We have adapted the model for seasonal use by having it read in instantaneous heliocentric distances and sub-solar latitude values calculated using the model from Dobrovolskis et al. (1997). These values are then used to take into account how Pluto's geometry relative to the sun changes throughout its orbit.

The model used here, of course, does have limitations. The thermophysical parameters are not temperature dependent, thermal re-radiation is only from the surface layer, and most importantly, volatiles are assumed to escape without re-condensing so that the temperatures of volatile ices can vary over the surface (the global model is treated in Section 2.3). Even with these limitations the model serves as a good starting point for understanding seasonal temperature variations on Pluto. For example with a homogeneous Pluto (assume global uniform albedo of 0.3) a substantial range of temperatures with seasonally dependent asymmetrical latitude distributions become readily apparent (Fig. 2, right column). Pluto is of course variegated; we address the non-uniform case below. It should be noted that this model and its associated figures (e.g. Fig. 3) should not be interpreted as hard and fast results so much as a limiting case describing the absence of volatile transport for exploratory comparison to an opposing limiting case that includes volatile transport.

2.2. Pluto albedo model

In order to account for Pluto's albedo variations we have created a simplified albedo map of Pluto (Fig. 4) that takes into account several of the major albedo units on Pluto's surface. We assume a static Pluto, in which the albedo units do not vary with time or with solar zenith angle. To represent the region informally known as Tombaugh Regio, we assign an albedo value of 0.6 to a patch 45° wide in longitude, and extending from −30° to 45° latitude. Elsewhere between ±25° latitude, we use a dark band with an albedo of 0.1 to represent the region informally known as Cthulhu Regio. At all other locations an albedo of 0.3 is assumed.

2.3. Global model

Most of the time Pluto's atmosphere may be in surface temperature equilibrium with surface frosts (Owen et al., 1993; Trafton, 1984). Along with our local model we also consider a global temperature model for comparison. By looking at how the temperatures of the local model compare with the instantaneous, global equilibrium temperatures we can get a better understanding of which regions will most likely be losing volatiles and which will be gaining volatile deposits.

Just as with the local model we start the global modeling using the heliocentric distance and sub-solar latitude calculated based on Dobrovolskis et al. (1997). Again we assume an emissivity of 0.9 based on Spencer et al. (1989). In order to avoid overlapping albedo regions in the model we simplify our albedo map to include poles, with an albedo of 0.3, which extend to ±45° and a bright patch with albedo 0.6 which extends from −30° to 45° and is 45° wide in longitude. All other areas on the surface are assumed to be depleted of volatiles. We can then calculate global temperatures based on the energy balance equations given in

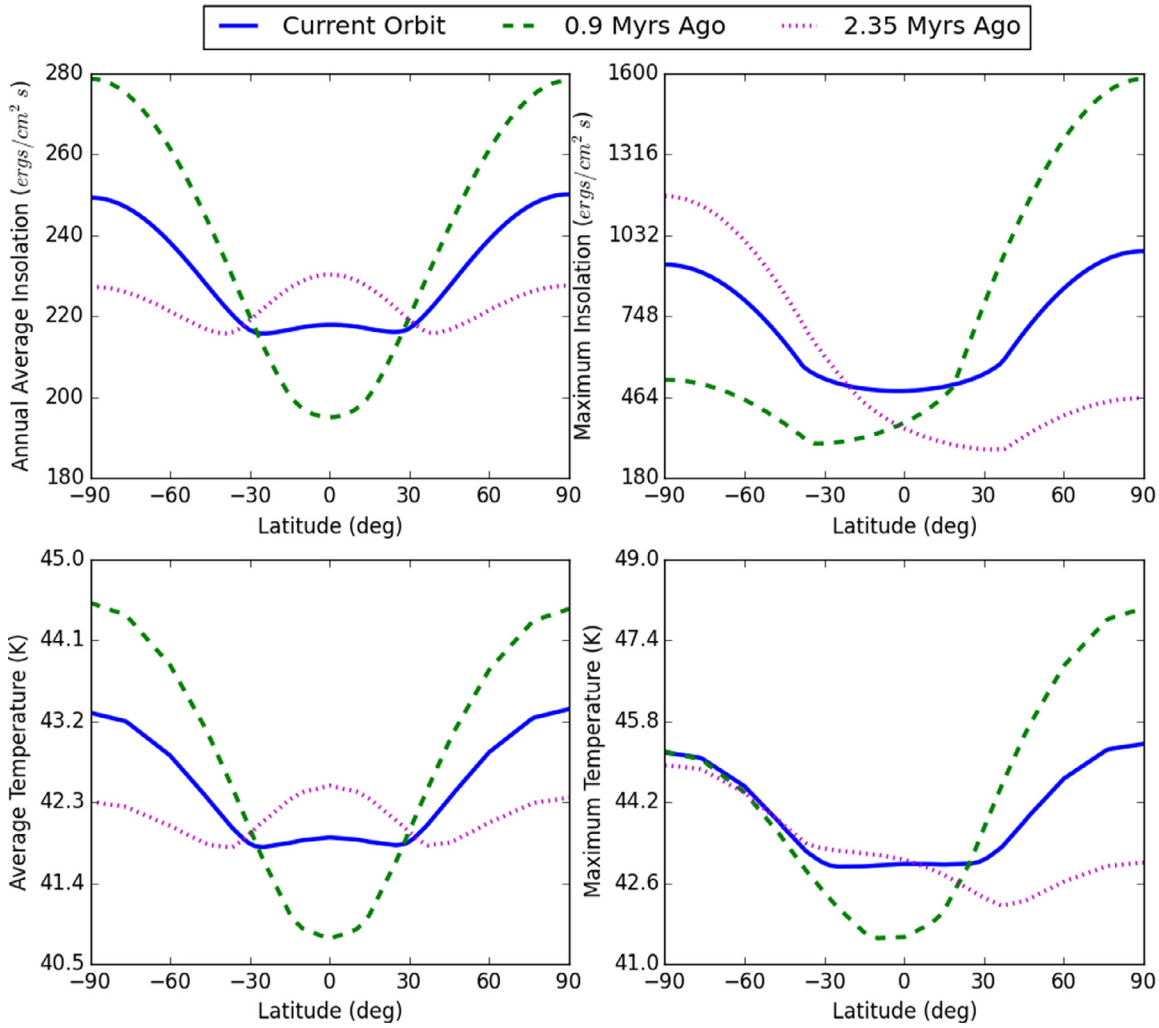

Fig. 2. Top Left: Average insolation over one Pluto orbit as a function of latitude. **Top Right:** Maximum insolation reached during one Pluto orbit as a function of latitude. **Bottom Left:** Average surface temperature over one Pluto orbit as a function of latitude. **Bottom Right:** Maximum surface temperature reached at each latitude over one Pluto orbit as a function of latitude. Blue, solid lines are over Pluto's current orbit. Green, dashed lines over one Pluto orbit, 0.9 million years ago, and the purple, dotted line over one Pluto orbit 2.35 million years ago. Note the changing y-axis scales. For the temperature profiles a global albedo of 0.3 is assumed. (For interpretation of the references to color in this figure legend, the reader is referred to the web version of this article.)

Trafton (1984). However, Eq. (10) in Trafton (1984) appears to contain an extra factor of A, which we removed. The original version also only accounts for polar caps as a volatile reservoir, we have modified it to include Tombaugh Regio as a volatile region. Our modified version of Trafton's energy balance equation is:

$$(A_{NP}+A_{SP}+A_{TR})\epsilon\sigma T^4 = \pi F_{\odot}[(1-a_P)(A^*_{NP}+A^*_{SP}) + (1-a_{TR})A^*_{TR}] \quad (1)$$

where ϵ is the emissivity, $\pi F_{\odot}$ is the solar flux at Pluto, a_i the albedo of the region, A_i the area of the region, and A_i^* the effective insolation area of the region. The subscript NP denotes the north polar region, SP the south polar region, and TR the bright equatorial region informally known as Tombaugh Regio (note: all features names are informal at this time).

Trafton (1984) also provides the equations necessary to calculate A^* for the polar regions. If a pole is in shadow, $A^* = 0$. If the pole is sunward facing and the sub-solar latitude (ϕ) is greater in magnitude than the colatitude of the polar cap boundary (θ_c or $\pi - \theta_c$) then $A^* = \pi \sin^3\phi$. For the in-between cases, where a pole is partially lit, the equation becomes more complicated:

$$A^* = \frac{\pi}{2} - \cos\theta_c\sqrt{\cos^2\phi - \cos^2\theta_c} - \cos^2\phi \sin^{-1}\left(\frac{\cos\theta_c}{\cos\phi}\right) + \sin\phi\sin^2\theta_c\cos^{-1}\left(-\frac{\tan\phi}{\tan\theta_c}\right) + \sin^2\phi\tan^{-1}\left(\frac{-\sec\phi}{\sqrt{\tan^2\theta_c - \tan^2\phi}}\right) \quad (2)$$

Eq. (2) is reproduced from Trafton's equation 13 (a full derivation can be found in Trafton, 1984). The $\cos^{-1}$ term is in the second quadrant when $\phi > 0$ and in the first quadrant when $\phi < 0$. To calculate the contribution from the opposite hemisphere (Trafton, 1984) uses $-\phi$ instead of ϕ.

We calculate A^* for the northern and southern part of Tombaugh Regio separately (and then add them). For each side we use the process described in the previous paragraph to determine A^* for the entire hemisphere as well as a cap reaching down to the extent of Tombaugh Regio in that hemisphere. By subtracting A^* of this cap from A^* of the entire hemisphere we are left with the latitudinal band on which Tombaugh Regio lies. We can then divide this band, based on the longitudinal width of Tombaugh Regio, to get A^* for just Tombaugh Regio.

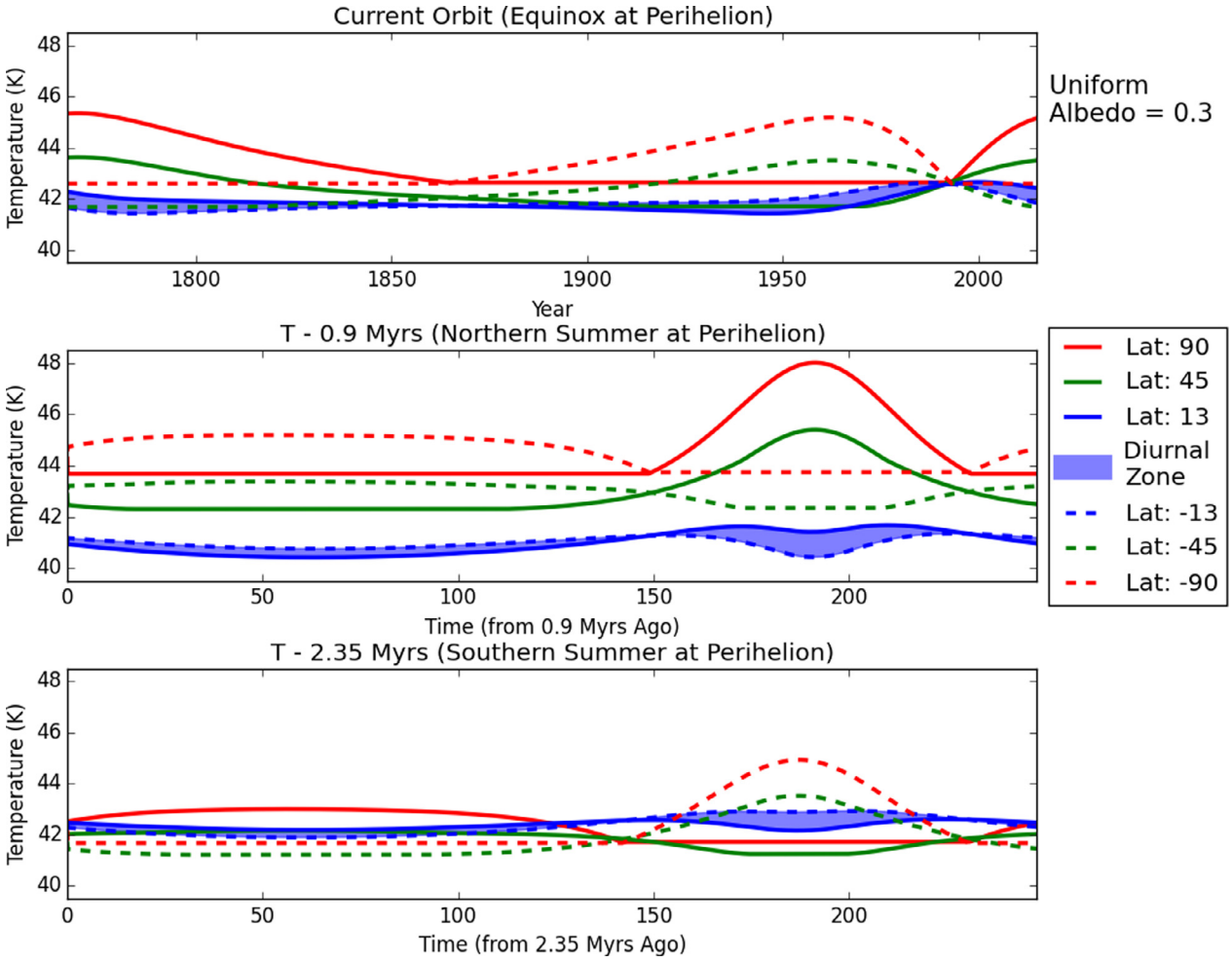

Fig. 3. Top: average daily surface temperatures over the past Pluto orbit. **Middle:** average daily surface temperatures over one Pluto orbit, 0.9 million years ago. **Bottom:** average daily surface temperatures over one Pluto orbit, 2.35 million years ago. Southern hemisphere latitudes are indicated by dashed lines while, Northern hemisphere by solid lines and the shaded region the "diurnal zone".

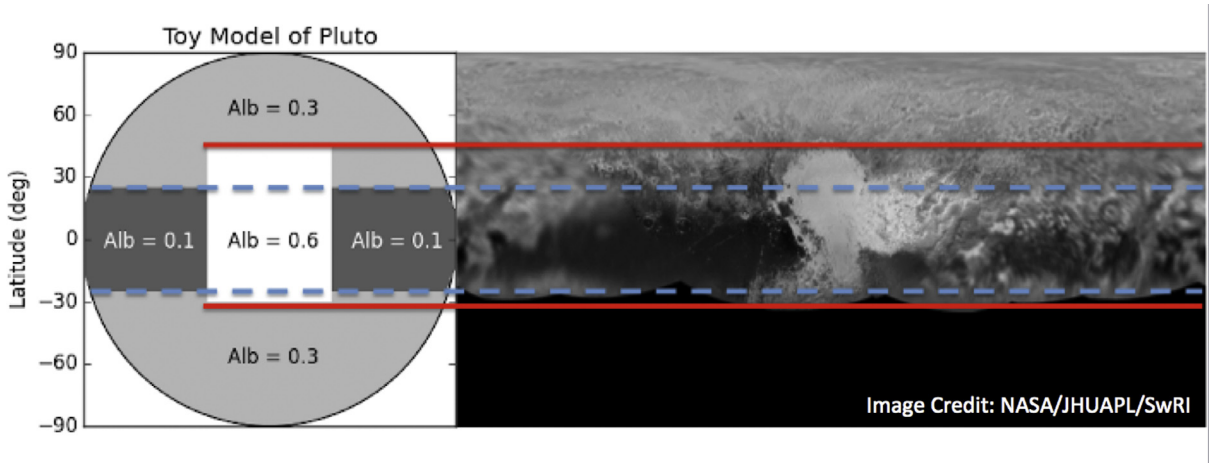

Fig. 4. Left: The simplified albedo map used for the local thermal modeling **Right:** Cylindrical mosaic of Pluto. The latitude ranges for the simplified albedo map have been estimated from the mosaic map of Pluto.

While this model provides us estimates of the global temperatures on Pluto that we can compare to our local temperatures model, this model does have limitations. Most notably, it does not take into account thermal inertia or internal heat flux. The temperatures provided by the model are instantaneous, and as a result drop below most of our local model temperatures when Pluto is at perihelion.

3. Results

3.1. Annual temperature patterns - uniform albedo model

We start our discussion by looking at local surface temperature variations at select latitudes over the course of one Pluto orbit for our three epochs of interest for the case of a globally uniform albedo of 0.3 across the entire surface. Fig. 3 shows temperature variations at the poles, ±45°, and in the "diurnal zone". We define the "diurnal zone" as the area between −13° south and +13° north. This is the region on Pluto's surface that always receives diurnal insolation as the obliquity varies over million year timescales (for further discussion of the "diurnal zone", see Binzel et al. (2017)). All other regions of Pluto have been in the arctic (or antarctic) circle at some point in the past few million years, experiencing long periods of constant sunlight in "summer" and constant darkness in "winter".

Looking at Fig. 3 we see obvious latitudinal variations as well as two changing trends between the three epochs: (1) the differences between polar, mid-latitude and equatorial surface temperatures vary between epochs and (2) the surface temperature patterns of the two hemispheres, specifically the poles, contrast within each epoch as well as when comparing them between epochs.

The difference between polar, mid-latitude and equatorial local surface temperatures from one epoch to the next are largely driven by how Pluto's obliquity (and as a result insolation patterns) are changing over million-year timescales. This can be seen by comparing the differences in Fig. 3 with the insolation curves in Fig. 2. Not surprisingly the areas receiving the highest average insolation over the year also experience the warmest surface temperatures. The interesting exception to this can be seen in the 2.35-million-year-ago case. During this epoch the equator receives a higher average insolation, however since it is in the "diurnal zone" the insolation is fairly evenly distributed throughout the year, leading to steady surface temperatures that are generally lower than the peak polar surface temperatures. This is caused by the poles receiving constant insolation as "midnight sun" for part of the year. The diurnal zone surface temperatures are generally the most steady (varying by only ∼0.5 K per year) while polar temperatures vary by 3 or more degrees throughout the year.

The other variations are the contrasts between the hemispheres during each Pluto year as well as the different epochs. These variations are driven primarily by variations in Pluto's sub-solar latitude at perihelion coupled with its relatively high orbital eccentricity ($e \approx 0.25$). During the current epoch, equinox and perihelion occur close together. As a consequence, the north pole receives insolation from roughly the time Pluto passes perihelion until it reaches aphelion while the south pole receives insolation from aphelion to perihelion. This results in both poles having equal length dark seasons and summers of similar duration and intensity. In contrast, 0.9 million years ago when Pluto's sub-solar latitude at perihelion was high in the northern hemisphere (at $\sim +76°$), the northern hemisphere received direct sunlight at perihelion while the southern hemisphere received its most direct sunlight at aphelion where the insolation flux is diminished by a factor of three. This results in what we are referring to as "Extreme Seasons", where one pole receives a short, "hot" summer and long winter, while the other receives a short winter and much longer, but less intense summer. A slightly less dramatic version of these "Extreme Seasons" can be seen in the epoch 2.35 million years ago when the sub-solar latitude at perihelion was $\sim -53°$ leading to short-lived high local surface temperatures in the southern hemisphere and a much longer, but lower temperature summer in the northern hemisphere. We emphasize since the equatorial region always receives its solar energy on a diurnal day/night cycle and never during an interval of continuous arctic summer, the equatorial region does not experience any "Extreme Seasons" the way the poles do.

Table 1
Minimum and maximum global temperature (K) reached for each epoch.

Epoch	Min T (K)	Max T (K)
Current	24.4	37.7
0.9 million years ago	27.5	45.0
2.35 million years ago	27.5	38.4

3.2. Historical temperature extremes - variegated albedo model

To get a more global view of trends on Pluto, and to incorporate Pluto's striking albedo variations we ran the thermal model for various latitude and albedo combinations (based on the simple albedo map we presented in Section 2.3 and shown in Fig. 4). From these trials we were able to create minimum and maximum local surface temperature maps (Fig. 5) to study how both albedo and latitude variations affect surface temperature extremes. The effects of the "Extreme Seasons" discussed in the previous subsection can be seen in these plots.

Fig. 5 draws attention to the impact albedo variations have on surface temperature. The bright, 0.6 albedo region, representing Tombaugh Regio stays cold (never rising above ∼37 K) while the darker, 0.1 albedo, Cthulhu Regio stays warmer (never falling below ∼42.5 K), even though these two regions are at comparable equatorial latitudes.

To get a better idea of long term extrema we took the information from the subplots presented in Fig. 5 and combined it to determine the absolute minimum and maximum temperature reached at each latitude and albedo combination over the three epochs of interest combined. These results can be seen in Fig. 6. This emphasizes the contrast between the bright region which generally never exceeds 40 K and the rest of Pluto where local surface temperatures never drop below 40 K and reach almost 50 K.

3.3. Comparison with global model

To gain a better understanding of what regions we expect to be experiencing sublimation and deposition we compare some of our local model results with the global temperature model described in Section 2.3. Since the global model does not account for thermal inertia we can make more direct comparisons by comparing the global temperatures to the instantaneous equilibrium temperatures calculated by the local model. We chose to focus on three specific latitudes: the north pole (90°), the equator (0°), and the south pole (−90°).

For each of the latitudes and epochs of interest we compare the instantaneous local temperature testing albedo values of 0.1, 0.3, and 0.6, with the global temperature over that same time period (Fig. 7). The minimum and maximum global temperature for each epoch are also given in Table 1. Since there is no thermal inertia the equatorial temperatures will vary considerably throughout a Pluto rotation, so here we just look at the mean equatorial equilibrium temperature over each Pluto rotation. We see some obvious contrasts between the polar and equatorial cases. The equatorial temperatures never vary by more than a few degrees Kelvin while

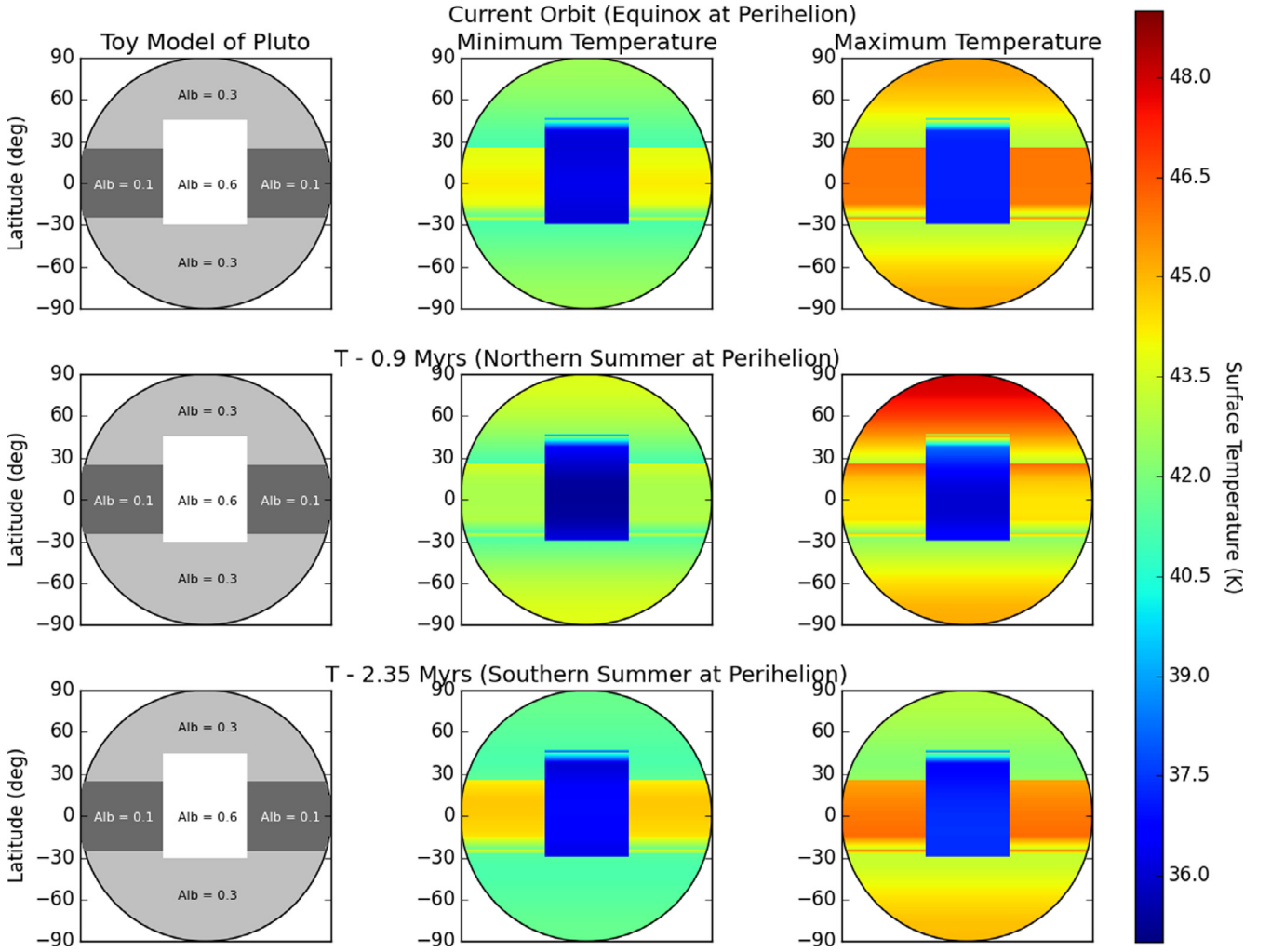

Fig. 5. This figure compares Pluto's current orbit with its past extreme seasons. **Left Column:** The simple albedo map of Pluto used to make local surface temperature maps. **Center Column:** The minimum temperature reached during the Pluto year for each latitude and albedo combination on Pluto's surface **Right Column:** The maximum temperature reached during the Pluto year for each latitude and albedo combination. **Top Row:** The current Pluto orbit **Middle Row:** One Pluto orbit, 0.9 million years in the past. **Bottom Row:** One Pluto orbit, 2.35 million years ago.

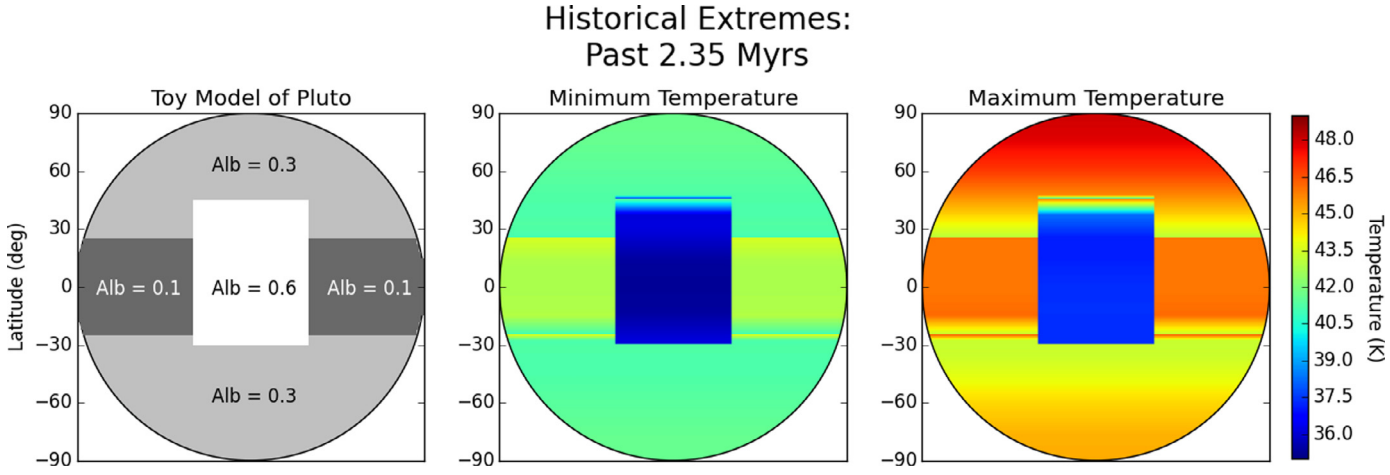

Fig. 6. Left: The simple albedo model of Pluto initially introduced in Section 2.2, used for the local model **Middle:** The minimum surface temperature reached at each latitude and albedo combination over the three epochs of interest **Right:** The maximum surface temperature reached at each latitude and albedo combination over the three epochs of interest.

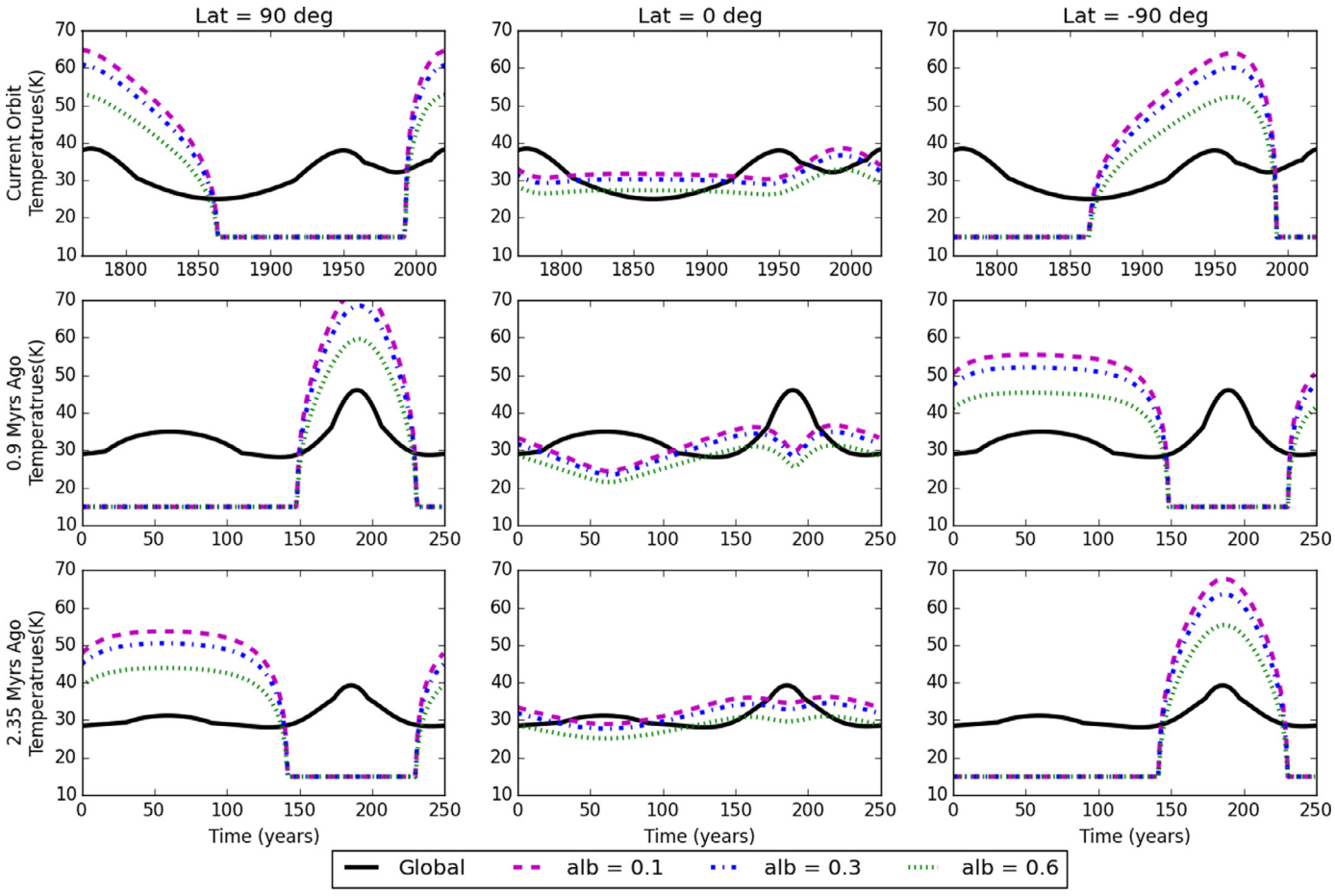

Fig. 7. Comparison of instantaneous global temperatures to instantaneous local equilibrium temperatures for select latitudes and albedos. The columns are organized by latitude with **left:** latitude 90°, **center:** latitude 0°, **right:** latitude −90°. The rows are organized by epoch with **top:** the current Pluto orbit (where the time increment is Earth years), **middle:** one Pluto orbit, 0.9 million years ago, **bottom:** one Pluto orbit, 2.35 million years ago. The global temperatures are indicated by the solid, black lines, the albedo = 0.1 local cases are purple, dashed lines, the albedo = 0.3 cases are blue, dot-dashed lines, and the albedo = 0.6 cases are marked with green, dotted lines. (For interpretation of the references to color in this figure legend, the reader is referred to the web version of this article.)

the polar temperatures show dramatic seasonal variations of 40 K or more. The global temperatures range between roughly 25 and −45 K, showing the greatest amplitude over the 0.9 million years ago epoch when Pluto was near its minimum obliquity.

4. Discussion

When considering long-term insolation patterns on Pluto, the relative minimum at the equator relative to the poles has been shown in several previous works (e.g. Dobrovolskis, 1989; van Hemelrijck, 1982, and Spencer et al., 1997) and illustrated at multiple epochs by Earle and Binzel (2015). Our analysis produces a bright equatorial band rather than a "spot" which Hamilton (2016, submitted) argues is created through a localized runaway albedo effect. We argue instead that the equatorial region on Pluto is a "preservation zone" for whatever is seeded there, where the preservation capability is driven by the coupling of the local albedo with an always diurnal cycle (and never a continuous arctic summer or winter), which we first showed qualitatively in Earle et al. (2015). *Thus the equatorial zone is optimized to be the region of maximum contrasts that allows the darkest region (Cthulhu Regio) to abut directly the brightest region (Sputnik Planitia).*

We find that once a region at the equator becomes bright it will become both the coldest and most consistently available cold trap, making it a likely area for volatile deposition, which in turn will refresh and brighten the surface. So for example, if Sputnik Planitia formed from an impact basin, as suggested by Moore et al. (2016), the topographic low would have initially attracted volatiles, creating a bright spot and triggering runaway volatile deposition in that area. Surface composition maps show that Tombaugh Regio is in fact volatile rich, showing high abundances of both N_2 and CH_4 (Grundy et al., 2016). In contrast, Cthulhu regio does not show any volatile abundances (Grundy et al., 2016). Given Cthulhu's low albedo and resulting higher local surface temperatures it could be expected that once a region at the equator began to darken it would become consistently one of the warmest regions of the planet and thus unlikely to gain any long term volatile accumulation, leading to further darkening.

Another way of looking at this effect is to compare the instantaneous equilibrium temperatures with the global temperatures, as we did in Fig. 7. The polar temperatures show dramatic seasonal variations, spending portions of the year well above and well below the global temperatures. This suggest these regions will undergo cycles of deposition and sublimation and their volatiles (or at least a portion of their volatiles) will be seasonal. This effect persists for all of the albedo cases we tested, suggesting the polar regions are not likely to experience runaway albedo variations. The equator on the other hand shows less seasonal variation, and remains close to the global temperature throughout the epochs studied. Over most of the time periods studied the bright (albedo = 0.6) equator temperatures are several degrees colder than the global temperature, it only briefly gets above the global temperature, and never by more than a few degrees, indicating net deposition is most likely occurring in bright equatorial regions.

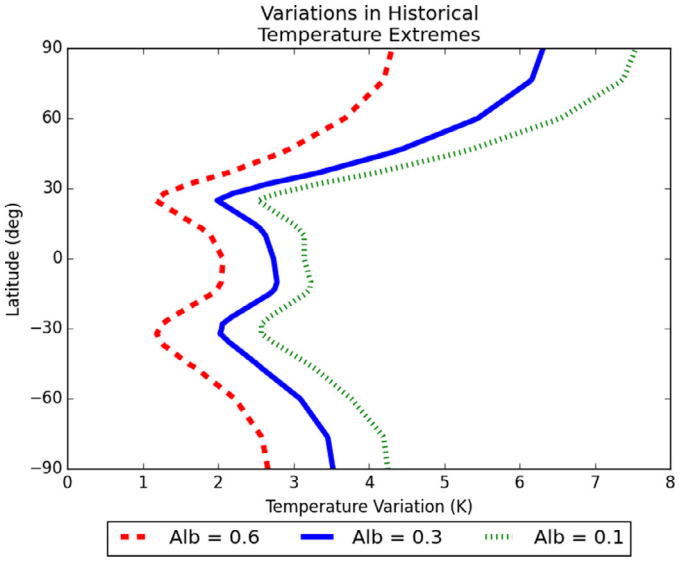

Fig. 8. Latitude on Pluto vs. the variation between the minimum and maximum temperature reached at that latitude considered over the three epochs of interest: the current orbit, 0.9 million years ago, and 2.35 million years ago. The red, dashed line uses an albedo of 0.6, the blue, solid line an albedo of 0.3, and the green, dotted line an albedo of 0.1. (For interpretation of the references to color in this figure legend, the reader is referred to the web version of this article.)

Such ongoing long-term net deposition could be an important factor that keeps Tombaugh Regio's morphology appearing 'young' and crater-free. On the other hand, the dark (albedo = 0.1) equator temperatures are generally higher than global temperatures, and only dip below the global temperatures for brief periods during each orbit. If all of the volatiles migrate away from a region, the bare surface will no longer be cooled by sublimation and a significant amount of seasonal cooling will need to take place before seasonally transient frosts can be deposited (Trafton, 1984). Taking this into consideration, it is very likely that dark, equatorial regions are generally bare of volatiles, any volatiles deposited are most likely minimal and seasonal. These comparisons show further evidence for runaway albedo variations at the equator and more stable, and spatially consistent albedos in the polar regions.

Thus the fact that the brightest and darkest regions on Pluto co-exist at the same latitude demonstrate that it is not the insolation minimum that drives the survival of Pluto's "cold icy heart". Rather it is the diurnal zone that allows self-preservation of an albedo extreme that gets seeded therein. To understand this phenomenon further we looked at the difference between the absolute maximum and absolute minimum local surface temperature reached at each latitude over the three epochs of interest, to see how much temperature variation each latitude experiences (Fig. 8). We find that regardless of albedo, the variations in the equatorial and midlatitude region stay small, less than 3.5 K. Moving away from the midlatitudes and towards the poles the variation in temperature increases. This effect is more dramatic in the northern hemisphere where the variation at the north pole is between 4.3 and 7.5 K depending on the albedo. The stability of temperatures in the equatorial band independent of albedo makes it likely that once seeded, albedo variations in the equatorial region will be able to survive million-year or longer timescales while the polar region will be more susceptible to changing albedos.

5. Conclusions

After performing thermal modeling to study surface temperature variations on Pluto as a function of latitude and albedo we see stark contrasts in the surface temperatures of high albedo regions (like Sputnik Planitia) and low albedo regions (like Cthulhu Regio) near the equator. Once seeded, a bright region at the equator will become the coldest cold trap on Pluto's surface, making it a likely location for further bright, fresh volatile deposition. In contrast, once an equatorial region begins to darken, its lower albedo will help it stay warm, making it an unlikely place for long term volatile deposits to form. We see that even with Pluto's varying orbit, the bright, volatile rich Tombaugh Regio should be able to survive on million-year timescales. This also appears to be a unique characteristic of Pluto's equatorial region, and we don't expect such stark albedo variations would be able to survive in the polar regions.

The New Horizons observations are allowing for the development of better albedo maps of Pluto. As these maps become available we will be able to take a more detailed look at the local surface temperature variations across Pluto's surface. The first look presented here already points to some interesting results, including the survival of Tombaugh Regio over million-year timescales.

Acknowledgments

We thank NASA for financial support of the New Horizons project, and we thank the entire New Horizons mission team for making the results of the flyby possible.

This work was supported in part by the NASA New Horizons mission to Pluto under SwRI Subcontract 299433Q.

The authors would like to thank Anthony Dobrovolskis for early discussion to help develop our understanding of the dynamical evolution of Pluto on a fundamental level, as well as sharing code based on his chapter, "Dynamics of the Pluto Charon Binary", from the 1997 Pluto and Charon textbook from The University of Arizona Press. The author would also like to thank Larry Trafton and another anonymous reviewer for useful feedback and suggestions.

References

Binzel, R., Earle, A., Buie, M., Young, L., Stern, S., Olkin, C., Ennico, K., Moore, J., Grundy, W., Weaver, H., M., L., R., L., 2017. Climate zones on pluto and charon. Icarus.

Buie, M.W., Grundy, W.M., Young, E.F., Young, L.A., Stern, S.A., 2010. Pluto and charon with the hubble space telescope. I. Monitoring global change and improved surface properties from light curves. Astrophys. J. 139, 1117–1127. doi:10.1088/0004-6256/139/3/1117.

Buie, M.W., Tholen, D.J., 1989. The surface albedo distribution of pluto. Icarus 79, 23–37. doi:10.1016/0019-1035(89)90105-X.

Dobrovolskis, A.R., 1989. Dynamics of pluto and charon. Geophys. Res. Lett. 16, 1217–1220. doi:10.1029/GL016i011p01217.

Dobrovolskis, A.R., Harris, A.W., 1983. The obliquity of pluto. Icarus 55, 231–235. doi:10.1016/0019-1035(83)90077-5.

Dobrovolskis, A.R., Peale, S.J., Harris, A.W., 1997. Dynamics of the Pluto-Charon Binary. In: Pluto and Charon. The University of Arizona Press, pp. 159–167.

Earle, A.M., Binzel, R.P., 2015. Pluto's insolation history: latitudinal variations and effects on atmospheric pressure. Icarus 250, 405–412. doi:10.1016/j.icarus.2014.12.028.

Earle, A.M., Binzel, R.P., Stern, S.A., Young, L.A., Buratti, B.J., Ennico, K., Grundy, W.M., Olkin, C.B., Spencer, J.R., Weaver, H.A., 2015. Correlating pluto's albedo distribution to long term insolation patterns. In: AAS/Division for Planetary Sciences Meeting Abstracts, p. 200.05.

Grundy, W.M., Binzel, R.P., Buratti, B.J., Cook, J.C., Cruikshank, D.P., Dalle Ore, C.M., Earle, A.M., Ennico, K., Howett, C.J., Lunsford, A.W., Olkin, C.B., Parker, A.H., Philippe, S., Protopapa, S., Reuter, D.C., Schmitt, B., Singer, K.N., Beyer, R.A., Buie, M.W., Cheng, A.F., Jennings, D.E., Linscott, I.R., Parker, J.W., Schenk, P.M., Spencer, J.R., Stansberry, J.A., Stern, S.A., Thoop, H.B., Tsang, C.C., Verbiscer, A.J., Weaver, H.A., Young, L.A., 2016. Surface compositions across pluto and charon. Science 351, 6279.

Grundy, W.M., Olkin, C.B., Young, L.A., Buie, M.W., Young, E.F., 2013. Near-infrared spectral monitoring of pluto's ices: spatial distribution and secular evolution. Icarus 223, 710–721. doi:10.1016/j.icarus.2013.01.019, arXiv:1301.6284.

Hamilton, D.P., Young, L.A., Stern, S.A., Moore, J.A., the New Horizons Geology and Geophysics Team, 2016. The rapid formation of Sputnik Planitia early in Pluto's history. In: Nature, p. 200.07. submitted.

Hansen, C.J., Paige, D.A., Young, L.A., 2015. Pluto's climate modeled with new observational constraints. Icarus 246, 183–191. doi:10.1016/j.icarus.2014.03.014.

van Hemelrijck, E., 1982. The insolation at pluto. Icarus 52, 560–564. doi:10.1016/0019-1035(82)90015-X.

Levine, J.S., Kraemer, D.R., Kuhn, W.R., 1977. Solar radiation incident on mars and the outer planets - latitudinal, seasonal, and atmospheric effects. Icarus 31, 136–145. doi:10.1016/0019-1035(77)90076-8.

Moore, J.M., McKinnon, W.B., Spencer, J.R., Howard, A.D., Schenk, P.M., Beyer, R.A., Nimmo, F., Singer, K.N., Umurhan, O.M., White, O.L., Stern, S.A., Ennico, K., Olkin, C.B., Weaver, H.A., Young, L.A., Binzel, R.P., Buie, M.W., Buratti, B.J., Cheng, A.F., Cruikshank, D.P., Grundy, W.M., Linscott, I.R., Reitsema, H.J., Reuter, D.C., Showalter, M.R., Bray, V.J., Chavez, C.L., Howett, C.J.A., Lauer, T.R., Lisse, C.M., Parker, A.H., Porter, S.B., Robbins, S.J., Runyon, K., Stryk, T., Throop, H.B., Tsang, C.C.C., Verbiscer, A.J., Zangari, A.M., Chaikin, A.L., Wilhelms, D.E., Bagenal, F., Gladstone, G.R., Andert, T., Andrews, J., Banks, M., Bauer, B., Bauman, J., Barnouin, O.S., Bedini, P., Beisser, K., Bhaskaran, S., Birath, E., Bird, M., Bogan, D.J., Bowman, A., Brozovic, M., Bryan, C., Buckley, M.R., Bushman, S.S., Calloway, A., Carcich, B., Conard, S., Conrad, C.A., Cook, J.C., Custodio, O.S., Ore, C.M.D., Deboy, C., Dischner, Z.J.B., Dumont, P., Earle, A.M., Elliott, H.A., Ercol, J., Ernst, C.M., Finley, T., Flanigan, S.H., Fountain, G., Freeze, M.J., Greathouse, T., Green, J.L., Guo, Y., Hahn, M., Hamilton, D.P., Hamilton, S.A., Hanley, J., Harch, A., Hart, H.M., Hersman, C.B., Hill, A., Hill, M.E., Hinson, D.P., Holdridge, M.E., Horanyi, M., Jackman, C., Jacobson, R.A., Jennings, D.E., Kammer, J.A., Kang, H.K., Kaufmann, D.E., Kollmann, P., Krimigis, S.M., Kusnierkiewicz, D., Lee, J.E., Lindstrom, K.L., Lunsford, A.W., Mallder, V.A., Martin, N., McComas, D.J., McNutt, R.L., Mehoke, D., Mehoke, T., Melin, E.D., Mutchler, M., Nelson, D., Nunez, J.I., Ocampo, A., Owen, W.M., Paetzold, M., Page, B., Parker, J.W., Pelletier, F., Peterson, J., Pinkine, N., Piquette, M., Protopapa, S., Redfern, J., Roberts, J.H., Rogers, G., Rose, D., Retherford, K.D., Ryschkewitsch, M.G., Schindhelm, E., Sepan, B., Soluri, M., Stanbridge, D., Steffl, A.J., Strobel, D.F., Summers, M.E., Szalay, J.R., Tapley, M., Taylor, A., Taylor, H., Tyler, G.L., Versteeg, M.H., Vincent, M., Webbert, R., Weidner, S., Weigle, G.E., Whittenburg, K., Williams, B.G., Williams, K., Williams, S., Woods, W.W., Zirnstein, E., 2016. The geology of pluto and charon through the eyes of new horizons. Science 351, 1284–1293. doi:10.1126/science.aad7055, arXiv:1604.05702.

Nadeau, A., McGehee, R., 2015. A simple method for calculating a planet's mean insolation by latitude. arXiv:1510.04542.

Olkin, C.B., Young, L.A., Borncamp, D., Pickles, A., Sicardy, B., Assafin, M., Bianco, F.B., Buie, M.W., de Oliveira, A.D., Gillon, M., French, R.G., Ramos Gomes, A., Jehin, E., Morales, N., Opitom, C., Ortiz, J.L., Maury, A., Norbury, M., Braga-Ribas, F., Smith, R., Wasserman, L.H., Young, E.F., Zacharias, M., Zacharias, N., 2015. Evidence that pluto's atmosphere does not collapse from occultations including the 2013 may 04 event. Icarus 246, 220–225. doi:10.1016/j.icarus.2014.03.026.

Owen, T.C., Roush, T.L., Cruikshank, D.P., Elliot, J.L., Young, L.A., de Bergh, C., Schmitt, B., Geballe, T.R., Brown, R.H., Bartholomew, M.J., 1993. Surface ices and the atmospheric composition of pluto. Science 261, 745–748. doi:10.1126/science.261.5122.745.

Spencer, J.R., Lebofsky, L.A., Sykes, M.V., 1989. Systematic biases in radiometric diameter determinations. Icarus 78, 337–354. doi:10.1016/0019-1035(89)90182-6.

Spencer, J.R., Moore, J.M., 1992. The influence of thermal inertia on temperatures and frost stability on triton. Icarus 99, 261–272. doi:10.1016/0019-1035(92)90145-W.

Spencer, J.R., Stansberry, J.A., Trafton, L.M., Young, E.F., Binzel, R.P., Croft, S.K., 1997. Volatile transport, seasonal cycles, and atmospheric dynamics on Pluto. In: Pluto and Charon. The University of Arizona Press, p. 435.

Stern, S.A., et al., 2015. The pluto system: initial results from its exploration by new horizons. Science 350, aad1815. doi:10.1126/science.aad1815, arXiv:1510.07704.

Sussman, G.J., Wisdom, J., 1988. Numerical evidence that the motion of pluto is chaotic. Science 241, 433–437. doi:10.1126/science.241.4864.433.

Sussman, G.J., Wisdom, J., 1992. Chaotic evolution of the solar system. Science 257, 56–62. doi:10.1126/science.257.5066.56.

Trafton, L., 1984. Large seasonal variations in triton's atmosphere. Icarus 58, 312–324. doi:10.1016/0019-1035(84)90048-4.

Young, E.F., Binzel, R.P., 1993. Comparative mapping of pluto's sub-charon hemisphere - three least squares models based on mutual event lightcurves. Icarus 102, 134–149. doi:10.1006/icar.1993.1038.

Young, L., Grundy, W.M., Binzel, R.P., Earle, A.M., Linscott, I.R., Hinson, D.P., Zangari, A.M., McKinnon, W.B., Stern, S.A., Weaver, H.A., Olkin, C.B., Ennico, K., Gladstone, G.R., Summers, M.E., Moore, J.M., Spencer, J.R., 2015. Volatile transport implications from the new horizons flyby of pluto. In: AAS/Division for Planetary Sciences Meeting Abstracts, p. 101.04.

Young, L.A., 2013. Pluto's seasons: new predictions for new horizons. Astron. J. 766, L22. doi:10.1088/2041-8205/766/2/L22, arXiv:1210.7778.